Turkish Journal of Electrical Engineering & Computer Sciences

http://journals.tubitak.gov.tr/elektrik/

Research Article

Turk J Elec Eng & Comp Sci
(2020) 28: 784 – 798

doi:10.3906/elk-1904-201

A multibeam subarrayed time-modulated linear array

Ugur YEŞİLYURT, Ihsan KANBAZ, Ertugrul AKSOY*
Department of Electrical and Electronics Engineering, Faculty of Engineering, Gazi University, Ankara, Turkey

Received: 29.04.2019 • **Accepted/Published Online:** 16.10.2019 • **Final Version:** 28.03.2020

Abstract: In conventional time-modulated arrays (TMAs), because of the usage of the RF-switch, harmonics are generated at multiples of the modulation frequency. In this study, the synthesis of time-modulated arrays has been analyzed for cognitive radio (CR) systems, in which these harmonics are suitably exploited for more efficient utilization of the spectrum. In order to accomplish the desired pattern at requested harmonic frequencies, a new excitation strategy with sinusoidal signals is proposed. The use of sinusoidal waveforms creates independent beams, allowing independent steering capability. Moreover, by utilizing the subarray structure, it is possible to have a smaller number of excitation functions in the hardware. It is shown by means of explanatory examples that the effectiveness of the proposed approach is due to free-adjustable beamforming, beam steering, and low complexity.

Key words: Time-modulated arrays, subarrayed antennas, sideband radiation, harmonic beamforming, beam steering, cognitive radio

1. Introduction

The growing requests for information and mobility have forced telecommunication technologies to be faster and more reliable. As a critical component of wireless systems, antennas play an important role to meet system requirements and increase the overall system performance. In addition to design parameters such as excitation amplitude, excitation phase, and the position of the array elements with respect to the phase center, the concept of time for antenna arrays has attracted attention as an additional degree of freedom [1]. By using high-speed RF switching, time-modulated arrays (TMAs) are designed for patterns with ultralow side lobe level (SLL) at the carrier frequency [2]. However, due to periodic switching of array elements, in addition to the main frequency component, undesired infinite harmonics, known as sideband radiation (SR), inevitably arise at multiple frequencies. The first research in this area shows that SR was regarded as power loss and the harmonics were successively suppressed. To improve the efficiency of suppressing harmonics, various optimization algorithms, such as differential evolution (DE), the genetic algorithm, and particle swarm optimization (PSO) and time-modulation strategies have been proposed [3–5]. Time-modulated strategies use various excitation schemes, namely variable aperture size (VAS), pulse shift (PS), pulse split (PsP), and variable pulse amplitude (VPA), via various optimization techniques [6–9]. It was shown in [10] that the shifting pulses of TMA changes the sideband radiations. In [11], sideband level suppression (SBL), sideband radiation suppression, and sideband bound suppression (SB) methods were analyzed for TMA. In [12], the closed form formulation for sideband radiation power and in [13] an inequality for the normalized maximum level of relative sideband level

*Correspondence: ertugrulaksoy@gazi.edu.tr

were derived. In addition, the sideband radiation power for a nonuniform time-modulated array (NTMA) was investigated in [14].

In ongoing research, harmonic radiation has been regarded as a benefit and these harmonics have been exploited to meet the communication system requirements, like direction finding, beam steering, and multiple-input multiple-output (MIMO) systems [15–19]. Hence, to achieve the basic goals of cognitive radio (CR), such as the efficient use of the spectrum and the reliability of the wireless communication systems, studies have focused on primary techniques such as harmonic beamforming and harmonic beam steering. More recently, to achieve these goals, a time-modulated phased array using a nonideal bipolar squared periodic sequence was proposed in [20] to form a single beam. The switched TMA architecture driven by periodic Nyquist pulsed signals provided the multibeam phased-array in [21]. Moreover, the amplitude modulation array, time-modulating sequences using the sum of weighted cosine (SWC) waveforms, and TMA with preprocessed rectangular sequences have been proposed in the literature [22–24]. In the periodical amplitude modulation in [22] and the time modulation sequences based on SWC pulses in [23], the beams occur at both positive and negative frequencies. Due to uncontrollable beams at the negative frequencies, beam steering ability is restricted. In TMA based on preprocessed rectangular sequences in [24], flexible beams are generated only at positive frequencies using periodic sinusoidal signals. However, these sinusoidal signals give rise to great complexity and cost in hardware. The other promising studies focused on beam synthesis are on frequency diverse arrays (FDAs) [25–27]. In this technique, the frequency of the carrier is incremented as a small change to generate range-dependent beams for different applications, especially radars.

The irregular array architectures including clustered, also called subarrayed, thinned, sparse, and time-modulated arrays, are reviewed in [28]. In clustered (namely subarrayed) arrays, the array elements are divided into cluster/subarrays with different sizes, orientations, or phases in order to reduce the control points such as amplifiers, phase shifters, and time-delay units. The subarrayed time modulated MIMO (STM-MIMO) antenna proposed in [29] uses a subarray structure, in which a certain number of array elements are placed in identical subarrays and each subarray is equipped with a high-speed Rf switch. In the TMA with the subarray proposed in [30], a group of the array element is placed in a particular configuration within the subarrays. In [30], the proposed structure, which is a simple and efficient array, consists of a combination of subarray and time-modulated array. The border element method (BEM) is used to provide a subarray configuration and PSO is exploited to optimize the pulse sequence in terms of minimization in both SR and SBL. A low complexity structure is obtained in which the normal and difference pattern in the main radiation and other harmonics are suppressed. In this study, a subarray structure similar to that in [28–30] has been proposed to reduce the complexity and provide a simple, effective, and efficient array architecture.

The conventional time-modulated arrays using high-speed RF switches have the drawback that multiple users cannot communicate independently in different directional beams at the same time. Since the switches are located just before the antennas, the user's signal is transmitted simultaneously from different beams of the same switch. This allows a signal to be transmitted in multiple directions rather than a single desired direction, and as a result, it is an issue for secure communication. In the proposed method, individual user signals can be transmitted independently in different harmonic beams by means of independent directional beams generated by the periodic sinusoidal signals.

In this paper, the synthesis of a subarrayed TMA, which is excited by a periodical sinusoidal waveform, is presented for the realization of CR systems. Unlike [22–24], in this study, the ability to create beams at the

desired harmonic frequencies instead of low-order harmonics provides additional flexibility to the system. As there are no uncontrollable beams at the negative harmonic frequencies, the beam steering capability increases and angular efficiency is obtained. Furthermore, in the system, when multiple users utilize the same antenna array, sinusoidal functions are located just before the antenna. These excitation functions lead to increased complexity and costs in the hardware part. To reduce this complexity, it is proposed that different users utilize different subarrays with fewer elements but with the same beam properties. In [17, 18], the radiation in the time-modulated array is used for direction-independent signal transmission, and it is a key advantageous point for secure communication. The proposed method can be considered as an enabling technology in which multiple users can be provided with independent and secure communication simultaneously in different spatial directions. Consequently, the proposed method can be added to studies on secure communication.

The rest of the paper is organized as follows. The theoretical derivations of the conventional TMA and the proposed periodical sinusoidal waveform are reviewed in Section 2. A new excitation concept driven by periodic sinusoidal functions to create independently adjustable beamforming is described in Section 3. Furthermore, to reduce the complexity and cost of the hardware, the proposed subarray structure is presented in detail. The numerical results in Section 4 and the comparisons with state-of-the-art studies in Section 5 are shown. Finally, conclusions are drawn in Section 6.

2. Background and proposed method

In the basic configuration, TMA is based on the principle of controlling the radiation pattern by periodically enabling and disabling the excitations of the individual array elements. For the TMA with N isotropic elements, located along the positive z-axis, the array factor is mathematically expressed as:

$$AF(\theta,t) = e^{jw_0 t}\sum_{n=1}^{N}\alpha_n F_n(t)e^{jkd_n\cos(\theta)}, \tag{1}$$

where α_n is the amplitude coefficient, $k = 2\pi/\lambda$ is the wave number at the center frequency, d_n is the position of the nth element with respect to the coordinate system origin, θ is the elevation angle with respect to z-axis, and $F_n(t)$ is the periodic switching function. The mathematical model of the conventional excitation switching approach, or variable aperture size (VAS), is expressed as:

$$F_n(t) = \begin{cases} 1 & , 0 < t \le t_n \le T_p \\ 0 & , \text{otherwise,} \end{cases} \tag{2}$$

where T_p denotes the switching period and t_n represents amplitude reversal time. Due to periodic switching, the corresponding modulation function $F_n(t)$ is decomposed into the complex Fourier series (CFS) and $F_n(t)$ is expressed as:

$$F_n(t) = \sum_{m=-\infty}^{\infty} C_{mn}e^{jmw_p t}, \tag{3}$$

where subscripts m, n, and C_{mn} respectively indicate the harmonic levels, the number of elements, and complex Fourier coefficients (CFC) of the nth element in the mth harmonic level. Substituting $F_n(t)$ values

into Equation (1), the array factor is expressed as:

$$AF(\theta,t)=\sum_{m=-\infty}^{\infty}\sum_{n=1}^{N}\alpha_n C_{mn}e^{jkd_n\cos(\theta)}e^{j(w_0+mw_p)t}. \tag{4}$$

In order to obtain the desired radiation pattern at the $w_0=2\pi f_0$ center operating frequency and w_0+mw_p harmonic frequencies $(w_p=2\pi f_p)$, the normalized pulse duration τ_n is an important parameter in the periodical (T_p) rectangular pulse. However, in order to suitably exploit harmonics $m\in\{\pm1,\pm2,\ldots\}$ in cognitive radio systems, this parameter alone is not sufficient. Hence, a new excitation strategy with the sinusoidal signal as an extra degree of freedom (DoF) is established as shown in Figure 1 and can be written as follows:

$$U_n(t)=F_n(t)+A_s\left[cos(w_st+\beta^n)+jsin(w_st+\beta^n)\right], \tag{5}$$

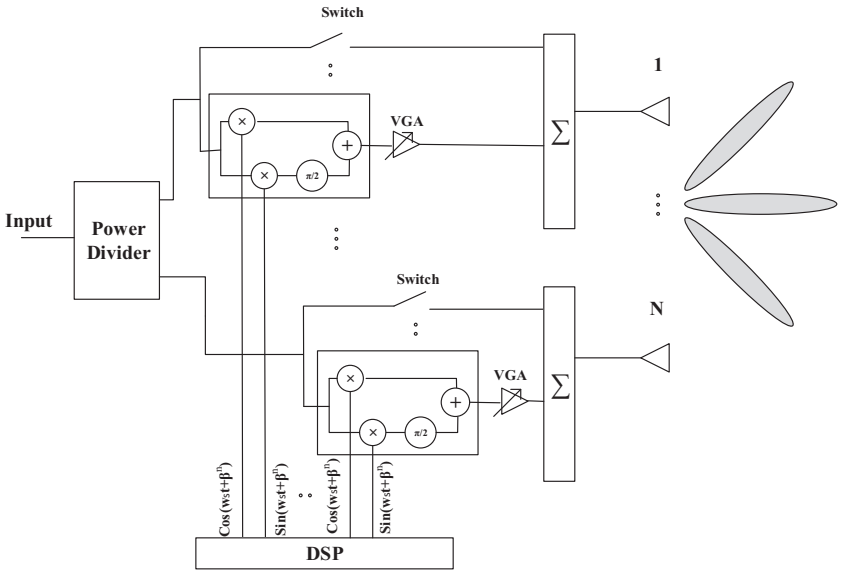

Figure 1. The TMA with periodical sinusoidal waveform.

where A_s, $w_s=2\pi f_s$, and β^n denote amplitude, frequency, and phase of the sinusoidal function, respectively. Because Fourier transforms of the sinusoidal function $F\{cos(2\pi f_st)+jsin(2\pi f_st)\}$ are $\delta(f-f_s)$, its Fourier coefficients occur only at $+f_s$ frequencies and not at other frequencies. Because of this feature of the sinusoidal signal, while the new excitation strategy does not change the main radiation, the sideband radiation (SR) depends on the frequency of the sinusoidal function. After the required calculation (see Appendix), C_{mn} CFC of the sinusoidal VAS for $m=0$ main radiation is defined as:

$$C_{0n}=\tau_n\,. \tag{6}$$

The CFCs for $m\neq0$ sideband radiations are obtained as:

$$C_{mn} = \frac{sin(m\pi\tau_n)}{m\pi} e^{-jm\pi\tau_n} + \frac{A_s}{2\pi(m - f_{rat})} \underbrace{\left(j[cos(2\pi f_{rat} + \beta^n) - cos(\beta^n)] + sin(\beta^n) - sin(2\pi f_{rat} + \beta^n) \right)}_{\phi}. \tag{7}$$

Here, $\tau_n = t_n/T_P$ and $f_{rat} = f_s/f_p$ represent the normalized switch-on duration and the ratio of the sine function frequency to the switching frequency, respectively. Under the conditions of $m \neq 0$, $m \neq f_{rat}$, and f_{rat} being an integer, with the help of total-difference formulas, the ϕ value in Equation (7) is equal to 0 and the new C_{mn} is $\frac{sin(m\pi\tau_n)}{m\pi} e^{-jm\pi\tau_n}$.

On the other hand, in the case of $m = f_{rat}$, the expression $\frac{A_s}{2\pi(m-f_{rat})}$ is undefined. A simple way to solve this issue is to assign $m = f_{rat}$ before the integration is complete. The sum of integrals $I_1 + I_2$ in Equation (23) can be reintegrated in the 0-T_p integral range as follows:

$$\frac{A_s}{T_p} \int_0^{T_p} [cos(w_s t + \beta^n) + j sin(w_s t + \beta^n)] \, e^{-jmw_p t} dt. \tag{8}$$

By using Euler's formula for the sinusoidal function, Equation (8) can be rewritten as:

$$I_1 + I_2 = \frac{A_s}{T_p} \int_0^{T_p} e^{j(w_s t + \beta^n)} e^{-jmw_p t} dt = \frac{A_s}{T_p} \int_0^{T_p} e^{j2\pi f_p (f_{rat} - m)t} e^{j\beta^n} dt. \tag{9}$$

In the case of $m = f_{rat}$, with some basic mathematical steps, Equation (9) can be rewritten as:

$$I_1 + I_2 = A_s e^{j\beta^n}. \tag{10}$$

Finally, under the far-field condition, integer f_{rat}, and $w_0/w_p \gg 1$ approximations, C_{mn} values can be expressed as:

$$C_{mn} = \begin{cases} \tau_n & ,m = 0 \\ \frac{sin(m\pi\tau_n)}{m\pi} e^{-jm\pi\tau_n} & ,m \neq 0, m \neq f_{rat} \\ \frac{sin(m\pi\tau_n)}{m\pi} e^{-jm\pi\tau_n} + A_s e^{j\beta^n} & ,m \neq 0, m = f_{rat} \end{cases}. \tag{11}$$

In the case of $m = f_{rat}$ (f_{rat}, harmonic frequency), component $A_s e^{j\beta^n}$ is formed but does not occur at other frequencies, and this component $A_s e^{j\beta^n}$ provides the flexibility to create an independent beam at the frequency. The switched TMAs are able to perform adaptive independent beamforming by adding sinusoidal waveforms at the desired harmonic frequencies. The beam steering in the beamforming design is an important aspect in terms of efficiency [31, 32]. The beam steering efficiency is related to the ability to obtain beamforming at each harmonic frequency and desired angle. Since there are no uncontrollable negative harmonic patterns, consistent with the single sideband structure [33], the proposed strategy increases the efficiency and flexibility.

3. Adaptive beamforming

In order to generate independently adjustable beamforming, the concept of nonswitched TMAs, which is driven by periodical sinusoidal functions, is proposed as shown in Figure 2. Let us consider a new waveform that

is the sum of the sine and cosine signal, $S_n(t) = \sum_{s=1}^{L} A_s \left[cos(2\pi f_s t + \beta_s^n) + jsin(2\pi f_s t + \beta_s^n)\right]$, and its the instantaneous array factor is

$$AF(\theta, t) = \sum_{n=1}^{N} \sum_{s=1}^{L} A_s \left[cos(2\pi f_s t + \beta_s^n) + jsin(2\pi f_s t + \beta_s^n)\right] e^{jkd_n \cos(\theta)}, \tag{12}$$

where L represents the number of harmonic frequencies used (or the number of users) and whose Fourier transform can be written as:

$$\widetilde{AF}(\theta, w) = \sum_{n=1}^{N} \sum_{s=1}^{L} A_s \delta(w_0 - w_s) e^{j\beta_s^n} e^{jkd_n \cos(\theta)}. \tag{13}$$

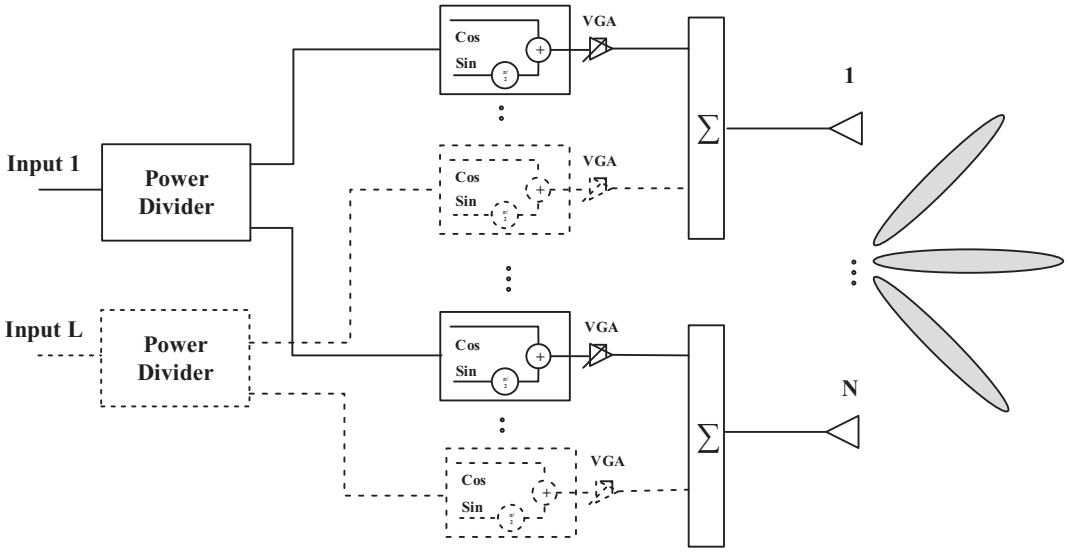

Figure 2. The nonswitched excitation strategy with sinusoidal signal.

In Equation (13), it is clear that AF is the value at $f_s(w_s = 2\pi f_s)$ frequencies, $s \in \{1, 2, ...L\}$, and the beam will occur at these frequencies. The SLL of the beam is directly adjusted according to a known or preoptimized distribution A_s. In addition, due to the progressive phase term β_s^n, the angular accuracy is easily achieved. The same array can also be used to transmit more than one signal at the same time because independent beams occur.

In the proposed method, when the L user uses the N-element array, NxL sinusoidal functions are generated, which increases the complexity and cost in the hardware. To reduce complexity, the subarray structure shown in Figure 3 is proposed. In order for subarrays to be the common phase reference center and to be symmetrical with respect to the phase center, an array with an odd number of elements $N = 2M + 1$ and with the distance d between the elements is considered. In this case, the new array factor expression is written as:

$$AF(\theta, t) = \sum_{n=-M}^{M} \sum_{s=1}^{L} A_s \left[cos(2\pi f_s t + \beta_s^n) + jsin(2\pi f_s t + \beta_s^n)\right] e^{jn(kd\cos(\theta))}, \tag{14}$$

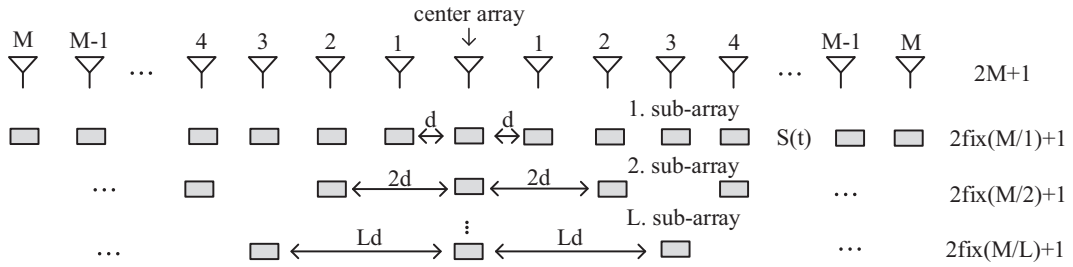

Figure 3. Sketch of the subarrayed and nonswitched TMAs only excited by periodical sinusoidal functions.

where the limits vary from –M to + M and the $d_n = d(n-1)$ expression changes to dn. Subarrays with a different number of elements are created, and these subarrays are allocated to different users. All of these subarrays have the same central array. The first user has a subarray structure including all the array elements ($N = 2M+1$) with the distance d between the elements. The second user has the subarray structure using the arrays at a distance of $2d$ to the right and left of the central array element. In this subarray, $2fix(M/2)+1$ array elements are used (fix rounds to the nearest integer toward zero). The third user has the subarray structure using the $2fix(M/3)+1$ array elements at a distance of $3d$ to the right and left of the central array element. Other users use subarrays created by this rule, respectively. The number of elements of each subarray is calculated by the following formula:

$$2fix\left(\frac{M}{s}\right)+1, \tag{15}$$

where s indicates which user it is. In the recommended structure, to reduce complexity, the number of sinusoidal functions required is obtained from the formula $\sum_{s=1}^{L} 2fix(M/s)+1$. In the subarray with the lowest element, i.e. with the highest spacing between the elements, the distance between the elements should be of a certain length ($Ld \leq 0.5\lambda$, not to be greater than 0.5λ). The number of elements decreases as the distance between the array elements increases in the subarrays. This feature ensures that the beam widths generated by each subarray are the same. In addition, since the number of elements in the subarrays outside the first subarray decreases, the number of sinusoidal functions used in the hardware decreases and the cost and complexity significantly reduce.

4. A numerical example

In this section, to illustrate the performance of the proposed method, three numerical examples are provided. Let us consider a 30-element linear array whose elements are located along the z-axis, the isotropic source with zero phases, and interelement spacing of $d = 0.5\lambda$. In the first simulation, the new excitation strategy with an RF switch is sampled. Using the differential evolution algorithm, the excitation time parameter of the switch in Figure 4 is determined so that –20 dB side lobe and –30 dB sideband levels are obtained. Sinusoidal signals with frequencies of $f_s = 5\,f_p$, $29\,f_p$, and $100\,f_p$ are added to create beams in the 5th, 29th, and 100th harmonic frequencies, respectively. The beams of the desired harmonics are aimed to be steered towards 33, 69, and 142 degrees in elevation. The expression $\frac{sin(m\pi\tau_n)}{m\pi}e^{-jm\pi\tau_n}$ is a very small value and converges to 0 in high-order

harmonics. Therefore, the term $A_s e^{j\beta^n}$ only remains and the progressive phase term may be defined as:

$$kd(n-1)cos\,(\theta_s) + (n-1)\beta_s^n = 0. \tag{16}$$

Once $\theta_1 = 33°, \theta_2 = 69°$, and $\theta_3 = 142°$ are considered, the excitation phases in classical phase array β_s^n are easily calculated by Equation (16). It can be clearly observed in Figure 5 that the beams of the desired harmonic frequencies can be steered to the specified directions without any distortion. The use of the desired harmonic frequencies provides flexibility and gives efficiency in angular accuracy.

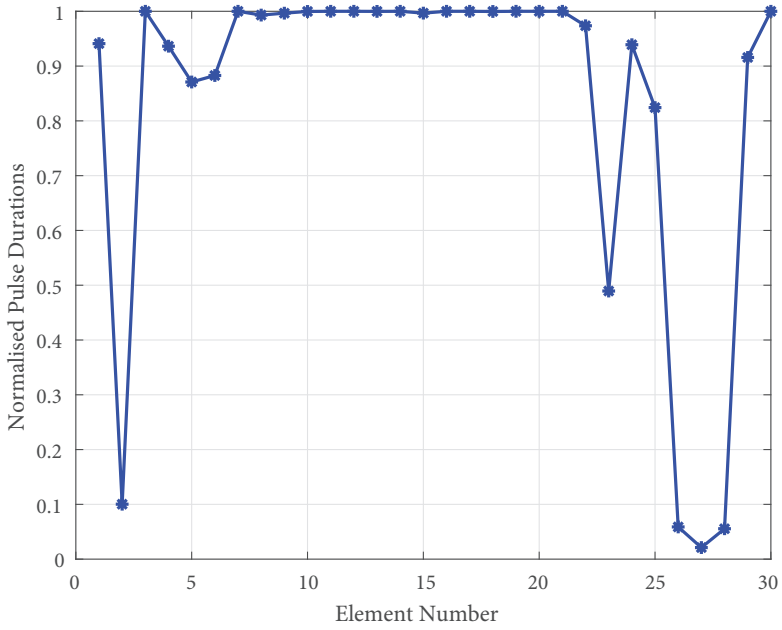

Figure 4. Normalized switch-on durations set with differential evolution algorithm to obtain –20 dB SLL and –30 dB SBL.

The second simulation relates to adaptive independent beamforming with a nonswitched new waveform. Since RF switches are not used, unwanted sidebands do not occur and less bandwidth is occupied. The spectrum is used more efficiently because only the frequencies needed are generated with the help of sinusoidal signals. Because the resulting beams are generated by independent signals, many users can communicate simultaneously using the same array. In addition, array silencing, which means that all elements are switched to the off position at any instant and prevents communication, does not occur. Suppose that three users (L = 3) communicate at $f = 13, 34, 105$ MHz frequencies and $\theta = 55, 92, 125$ degrees, respectively. It can be inferred from Figure 6 that a large number of signals can simultaneously be transmitted over the same antenna array, thanks to the independently adjustable beam.

In order to use fewer sinusoidal signals, the performance of the proposed subarray structure is investigated in the final simulation. Toward this aim, let us consider a 31-element linear array with interelement spacing of $d = 0.18\lambda$. Suppose that L = 3 signals are transmitted at the same frequency and angle values in the second example, respectively. Since all array elements are used for the first signal, the 31-element sinusoidal function is required. For the second signal using the second subarray structure, 15 functions are required and, finally, the third subarray is equipped with 11 sinusoidal functions. It is shown in Figure 7 that the same radiation patterns are obtained by using a total of 57 excitation signals instead of $3 \times 31 = 93$ in the proposed subarray

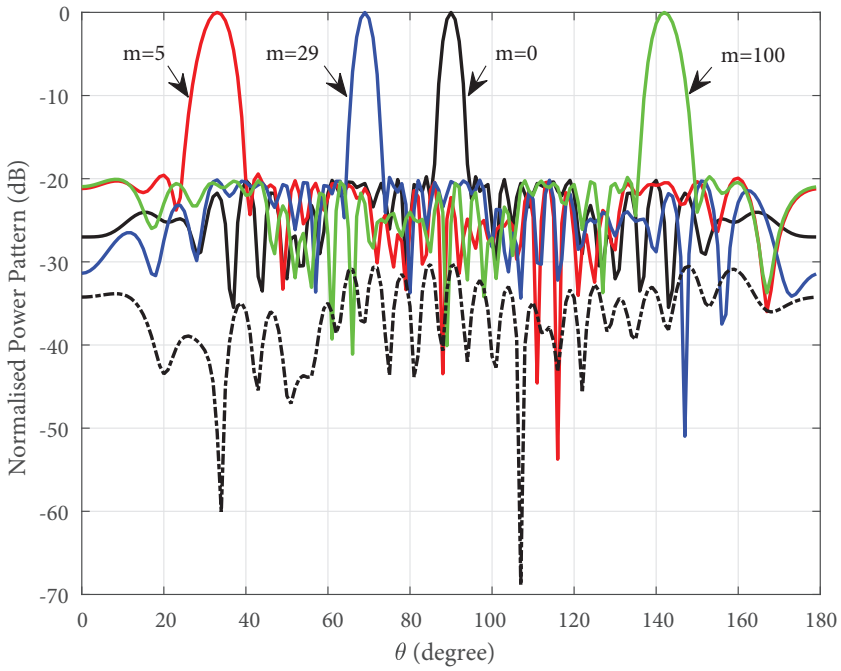

Figure 5. The radiation pattern of the TMA with periodical sinusoidal waveform. In order to obtain –20 dB SLL and –30 dB SBL, the excitation parameter of the switches is set by the differential evolution algorithm. Beamforming $\theta_1 = 33^\circ$, $\theta_2 = 69^\circ$, and $\theta_3 = 142^\circ$ over 5th, 29th, and 100th harmonic frequencies.

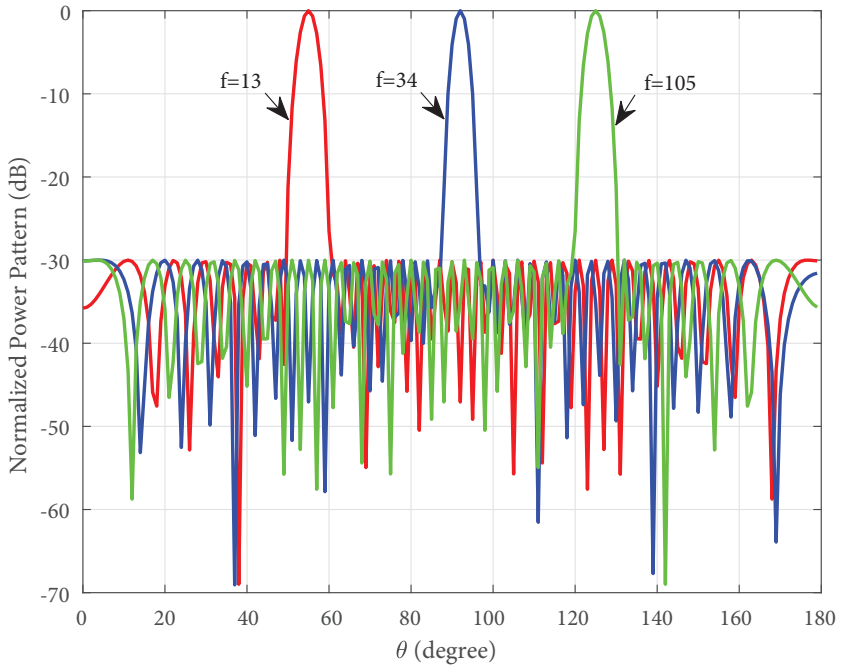

Figure 6. The radiation pattern of the nonswitched TMA with –30 dB Chebyshev amplitude condition. Beamforming $\theta_1 = 55^\circ$, $\theta_2 = 92^\circ$, and $\theta_3 = 125^\circ$ over $f = 13, 34, 105$ MHz frequencies.

structure. An improvement of 38.7% is achieved in complexity with the proposed subarray structure. In the nonswitched sinusoidal excitation structure, while the beam steering can be adjusted from 25 to 155 degrees, the beam steerable range in the subarrayed and the nonswitched sinusoidal excitation structure is between 45 and 135 degrees. As a result, it can be seen from the examples that the proposed method can perform independent beams and the steering of overall harmonics frequencies.

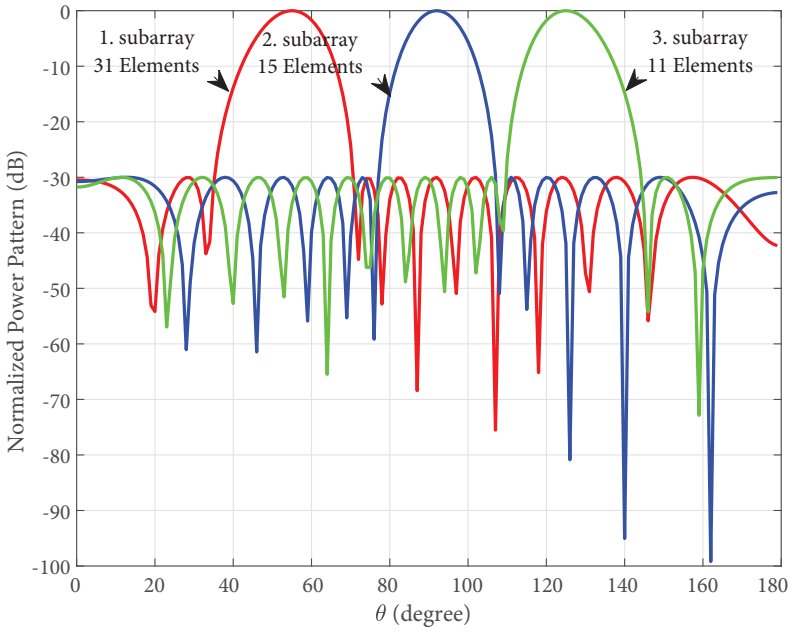

Figure 7. The radiation pattern of the subarrayed and nonswitched TMA with –30 dB Chebyshev amplitude condition. Beamforming $\theta_1 = 55^\circ$, $\theta_2 = 92^\circ$, and $\theta_3 = 125^\circ$ over $f = 13, 34, 105$ MHz frequencies.

5. Performance comparison with the state-of-the-art studies in terms of beamforming

The sideband radiations derived from the periodic time modulation need to be edited for beneficial purposes. Toward this aim, the effectiveness of the proposed method has been compared with the existing studies in the literature in terms of the beam scanning, SLL, SBL, and signal bandwidth limitations in the Table.

To determine phase-only weights, the single-sideband (SSB) TMA using the rectangular and trapezoidal pulses was proposed in [33]. The beam radiation on the fundamental harmonic component with about –13 dB SLL has been obtained. When the rectangular pulses and trapezoidal pulses with normalized rise/fall times of 1/15 and 1/6 are used, the peak value of the most important undesirable harmonic is –13.98 dB, –15.57 dB, and –27.98 dB, respectively. The switching frequency f_p and the signal bandwidth B_s should provide the $4f_p > B_s$ condition that the spectrum does not overlap.

As another approach for harmonic beamforming, the sum of weighted cosine (SWC) pulses has been proposed to flexibly window the harmonics in [23]. With the help of the SWC pulse coefficients, the SLL of the main, first, and second harmonic radiation is –35 dB, –22 dB, and –27 dB, respectively. The peak value of the most important undesirable harmonic is –25 dB, and the beamforming is performed on low-order harmonics or the harmonic cluster. Moreover, in order to generate the desired multiple patterns at a different harmonic frequency, an optimization strategy based on the particle swarm (PS) algorithm was proposed in [18, 34]. By determining the periodic time sequences with an optimization-based technique, the broadside sum, and

Table . Performance comparison of harmonic beamforming.

Ref.	Beam scanning	SLL (dB)	SBL (dB)	Constraint for B_s
[33]	Single beam (q=1)	-13	-13.98 (rect. pulse)	$4f_p \geq B_s$
		-13	-15,57 (trap. pulse $\delta/T_p = 1/15$) -27,98 (trap. pulse $\delta/T_p = 1/6$)	
[23]	Multibeam (q=1,2,3)	-35 (q=0) -22 (q=1) -27 (q=2)	-25	$f_p \geq B_s$
[34]	Multibeam (q=1,2,3)	-21.6 (q=0) -20 (q=1) -20 (q=2)	-	$f_p \geq B_s$
[18]	Multibeam (q=1,2,3)	-22.9 (q=0) -22.8 (q=1) -22.4 (q=2)	-	$f_p \geq B_s$
[35]	Single beam (q=1)	-20	-25	$(2p)f_p \geq B_s$
Proposed	Beam at desired harmonic frequency	-30, flexible adjustable	No harmonics	$(f_{s1} - f_{s2}) \geq B_s$

difference pattern, flat-top and narrow beams are also provided at both the main and fundamental harmonic radiations [34]. The SLL of the main and fundamental harmonics (∓ 1) radiations are –21.6 dB, –20 dB, and –20 dB, respectively, and the fundamental harmonics (∓ 1) are directed toward $+30$ and -30 degrees in elevation (fig. 8 in [34]). Moreover, the SLL of the main and the first two harmonic radiation is –22.9 dB, –22.8 dB, and –22.4 dB, respectively, directed 90, 116, and 150 degrees in elevation (fig. 11 in [18]). Besides, the peak values of the main and the first two harmonic radiations are –0 dB, –0.2 dB, and –0.8 dB. In [18, 23, 34], the relationship between the time modulation frequency f_p and the signal bandwidth B_s must satisfy the state of $f_p > B_s$ to avoid overlapping of the modulated signal.

In another harmonic beamforming approach, in order to realize amplitude and phase weightings in terms of the harmonic beamforming, time-modulated amplitude-phase weighting with multiple branches (TMAPW-MB) was proposed in [35]. The single-beam radiation with –20 dB SLL and –25 dB SBL on the fundamental harmonic component is provided through the proposed weighting technique. By using the proposed branches method with a fixed delay line, the even harmonic radiation components are suppressed and only odd harmonic radiation components remain. The switching frequency f_p and the signal bandwidth B_s should provide the $(2p)f_p \geq B_s$ condition to prevent aliasing effects in the spectrum, where p (i.e. $p = 2^k$, $k \in \mathbb{N}$) indicates the number of branches.

In this study, with the help of the proposed periodic sinusoidal signals, the ability to generate independent beam at the desired harmonic frequency is analyzed. The SLL of the independent beams generated is directly controlled by the amplitude values of the sinusoidal signals (e.g., Chebyshev distribution). The advantage of the proposed method is that no harmonics are generated as RF switches are not used. Furthermore, in the proposed method, there is an $(f_{s1} - f_{s2}) \geq B_s$ relationship between the modulation frequency f_s and the signal bandwidth B_s, where f_{s1} and f_{s2} are the frequency values of two independent beams (e.g., $f_{s1} = 13f_p$, $f_{s1} = 34f_p$ in Figure 6). This provides an advantage that leads to high bandwidth.

6. Conclusion

In this study, the synthesis of TMAs has been assessed in CR systems that enable more efficient utilization of the spectrum. The nonswitched periodic excitation waveform is introduced as an alternative excitation scheme both to boost and to steer harmonics. Compared to existing TMAs based on rectangular pulses, the proposed system only generates the desired harmonic frequencies and therefore occupies less bandwidth. In addition, it is observed that the number of required excitation signals is greatly reduced with the help of the proposed subarray scheme. The proposed method provides independent beamforming flexibility and spatial efficiency, which steer these beams to every angle. Consequently, due to the advantages of the proposed approach for adaptive harmonic beamforming, the proposed method can be considered for CR applications.

7. Appendix

The complex Fourier coefficients of sinusoidal VAS are calculated with:

$$C_{mn} = \frac{1}{T_p}\int_{-\infty}^{\infty}\left[F_n(t) + A_s\left(cos(w_s t+\beta^n) + jsin(w_s t+\beta^n)\right)\right]e^{-jmw_p t}dt. \tag{17}$$

For $m = 0$:

$$C_{0n} = \frac{1}{T_p}\int_{0}^{t_n}\left[1+A_s\left(cos(w_s t+\beta^n)+jsin(w_s t+\beta^n)\right)\right]dt+\frac{1}{T_p}\int_{t_n}^{T_P}\left[0+A_s\left(cos(w_s t+\beta^n)+jsin(w_s t+\beta^n)\right)\right]dt. \tag{18}$$

$$C_{0n} = \frac{1}{T_p}\left[t+\frac{A_s}{w_s}sin(w_s t+\beta^n) - \frac{jA_s}{w_s}cos(w_s t+\beta^n)\right]\Big|_{0}^{t_n} + \frac{1}{T_p}\left[\frac{A_s}{w_s}sin(w_s t+\beta^n) - \frac{jA_s}{w_s}cos(w_s t+\beta^n)\right]\Big|_{t_n}^{T_p}. \tag{19}$$

After some simple manipulations, C_{0n} may be written as:

$$C_{0n} = \frac{1}{T_p}\left[t_n - \frac{A_s}{w_s}sin(\beta^n) + j\frac{A_s}{w_s}cos(\beta^n) + \frac{A_s}{w_s}sin(w_s T_p+\beta^n) - j\frac{A_s}{w_s}cos(w_s T_p+\beta^n)\right]. \tag{20}$$

From the total-difference formulas,[1] $cos(2\pi f_{rat}+\beta^n)$ can be written as $cos(2\pi f_{rat})cos(\beta^n) - sin(2\pi f_{rat})sin(\beta^n)$. Because f_{rat} is an integer, $cos(2\pi f_{rat}) = 1$ and $sin(2\pi f_{rat}) = 0$ and the consequence of $cos(2\pi f_{rat}+\beta^n)$ is $cos(\beta^n)$. In the same way, $sin(2\pi f_{rat}+\beta^n)$ is equal to $sin(\beta^n)$. With the help of these conversion formulas, C_{0n} can be written again as:

$$C_{0n} = t_n/T_P = \tau_n\,. \tag{21}$$

For $m \neq 0$:

$$\begin{aligned} C_{mn} = {} & \frac{1}{T_p}\int_{0}^{t_n}\left[1+A_s\left(cos(w_s t+\beta^n)+jsin(w_s t+\beta^n)\right)\right].e^{-jmw_p t}dt \\ & +\frac{1}{T_p}\int_{t_n}^{T_P}\left[0+A_s\left(cos(w_s t+\beta^n)+jsin(w_s t+\beta^n)\right)\right].e^{-jmw_p t}dt. \end{aligned} \tag{22}$$

[1] The addition laws for cosine and sine functions: $cos(\theta_1+\theta_2) = cos\theta_1.cos\theta_2 - sin\theta_1.sin\theta_2$, $sin(\theta_1+\theta_2) = sin\theta_1.cos\theta_2 + cos\theta_1.sin\theta_2$

The C_{mn} expression can be written as the sum of I, I_1, and I_2 and is given by

$$\underbrace{\frac{1}{T_p}\int_0^{t_n} e^{-jmw_pt}dt = \frac{sin(\pi m\tau_n)}{m\tau_n}e^{-j\pi m\tau_n}}_{I} + \underbrace{\frac{A_s}{T_p}\int_0^{t_n}\left(cos(w_st+\beta^n)+jsin(w_st+\beta^n)\right)e^{-jmw_pt}dt}_{I_1} + \underbrace{\frac{A_s}{T_p}\int_{t_n}^{T_p}\left(cos(w_st+\beta^n)+jsin(w_st+\beta^n)\right)e^{-jmw_pt}dt}_{I_2}. \quad (23)$$

With the help of the $\int udv = uv - \int vdu$ integral transformation formula, the integral in the I_1 and I_2 expressions can be written as:

$$K = \frac{e^{-jmw_pt}}{m^2w_p^2 - w_s^2}\Big[j(mw_p+w_s)cos(w_st+\beta^n) - (mw_p+w_s)sin(w_st+\beta^n)\Big]. \quad (24)$$

The K value is written in the integral boundaries and the sum of I_1 and I_2 is obtained from

$$I_1 + I_2 = \frac{A_s}{T_p}K\Big|_0^{t_n} + \frac{A_s}{T_p}K\Big|_{t_n}^{T_P}. \quad (25)$$

After some basic mathematical transformations such as $f_{rat} = f_s/f_p$ and operations, the $I_1 + I_2$ total expression can be expressed as follows:

$$I_1 + I_2 = \frac{A_s}{2\pi(m - f_{rat})}\Big(j[cos(2\pi f_{rat}+\beta^n) - cos(\beta^n)] + sin(\beta^n) - sin(2\pi f_{rat}+\beta^n)\Big). \quad (26)$$

References

[1] Shanks HE, Bickmore RW. Four-dimensional electromagnetic radiators. Canadian Journal of Physics 1959; 37: 263. doi: 10.1139/p59-031

[2] Kummer W, Villeneuve A, Fong T, Terrio F. Ultra-low sidelobes from time-modulated arrays. IEEE Transactions on Antennas and Propagation 1963; 11 (6): 633-639. doi: 10.1109/TAP.1963.1138102

[3] Yang S, Gan YB, Qing A. Sideband suppression in time-modulated linear arrays by the differential evolution algorithm. IEEE Antennas and Wireless Propagation Letters 2002; 1: 173-175. doi: 10.1109/LAWP.2002.807789

[4] Yang S, Gan YB, Qing A, Tan PK. Design of a uniform amplitude time modulated linear array with optimized time sequences. IEEE Transactions on Antennas and Propagation 2005; 53 (7): 2337-2339. doi: 10.1109/TAP.2005.850765

[5] Poli L, Rocca P, Manica L, Massa A. Handling sideband radiations in time-modulated arrays through particle swarm optimization. IEEE Transactions on Antennas and Propagation 2010; 58 (4): 1408-1411. doi: 10.1109/TAP.2010.2041165

[6] Bekele ET, Poli L, Rocca P, D'Urso M, Massa A. Pulse-shaping strategy for time modulated arrays - analysis and design. IEEE Transactions on Antennas and Propagation 2013; 61 (7): 3525-3537. doi: 10.1109/TAP.2013.2256096

[7] Aksoy E, Afacan E. Sideband level suppression improvement via splitting pulses in time modulated arrays under static fundamental radiation. In: Electromagnetics Research Symposium (PIERS'2011); Suzhou, China; 2011. pp. 364-367.

[8] Aksoy E. Time modulation through variable pulse amplitude in 4D arrays. In: 13th International Conference on Telecommunications and Informatics (TELE-INFO '14); Istanbul, Turkey; 2014. pp. 12-21.

[9] Aksoy E, Afacan E. Thinned nonuniform amplitude time-modulated linear arrays. IEEE Antennas and Wireless Propagation Letters 2010; 9: 514-517. doi: 10.1109/LAWP.2010.2051312

[10] Aksoy E, Afacan E. Calculation of sideband power radiation in time-modulated arrays with asymmetrically positioned pulses. IEEE Antennas and Wireless Propagation Letters 2012; 11: 133-136. doi: 10.1109/LAWP.2012.2185916

[11] Aksoy E, Afacan E. A comparative study on sideband optimization in time-modulated arrays. International Journal of Antennas and Propagation 2014; 2014: 290737. doi: 10.1155/2014/290737

[12] Aksoy E. Calculation of sideband radiations in time-modulated volumetric arrays and generalization of the power equation. IEEE Transactions on Antennas and Propagation 2014; 62 (9): 4856-4860. doi: 10.1109/TAP.2014.2332004

[13] Aksoy E, Afacan E. An inequality for the calculation of relative maximum sideband level in time-modulated linear and planar arrays. IEEE Transactions on Antennas and Propagation 2014; 62 (6): 3392-3397. doi: 10.1109/TAP.2014.2311470

[14] Kanbaz I, Yesilyurt U, Aksoy E. A study on harmonic power calculation for nonuniform period linear time modulated arrays. IEEE Antennas and Wireless Propagation Letters 2018; 17 (12): 2369-2373. doi: 10.1109/LAWP.2018.2875530

[15] Ni D, Yang S, Chen Y, Yang F. Direction finding based on TMAs with reconfigurable angle-searching range and bearing accuracy. Electronics Letters 2017; 53 (3): 130–132. doi: 10.1049/el.2016.3932

[16] Tennant A. Experimental two-element time-modulated direction finding array. IEEE Transactions on Antennas and Propagation 2010; 58 (3): 986-988. doi: 10.1109/TAP.2009.2039301

[17] Zhu Q, Yang S, Yao R, Nie Z. Directional modulation based on 4-D antenna arrays. IEEE Transactions on Antennas and Propagation 2014; 62 (2): 621-628. doi: 10.1109/TAP.2013.2290122

[18] Rocca P, Zhu Q, Bekele ET, Yang S, Massa A. 4-D arrays as enabling technology for cognitive radio systems. IEEE Transactions on Antennas and Propagation 2014; 62 (3): 1102-1116. doi: 10.1109/TAP.2013.2288109

[19] Poli L, Rocca P, Oliveri G, Chuan M, Mazzucco C et al. Advanced pulse sequence design in time-modulated arrays for cognitive radio. IEEE Antennas and Wireless Propagation Letters 2018; 17 (5): 898-902. doi: 10.1109/LAWP.2018.2821715

[20] Maneiro-Catoira R, Bregains J, Garcia-Naya JA, Castedo L. Time-modulated phased array controlled with nonideal bipolar squared periodic sequences. IEEE Antennas and Wireless Propagation Letters 2019; 18 (2): 407-411. doi: 10.1109/LAWP.2019.2892657

[21] Maneiro-Catoira R, Bregains J, Garcia-Naya JA, Castedo L. Time-modulated multibeam phased arrays with periodic Nyquist pulses. IEEE Antennas and Wireless Propagation Letters 2018; 17 (12): 2508-2512. doi: 10.1109/LAWP.2018.2880087

[22] He C, Cao A, Liang X, Jin R, Geng J. Beamforming method with periodical amplitude modulation array. In: 2013 IEEE Antennas and Propagation Society International Symposium (APSURSI); Orlando, FL, USA; 2013. pp. 874-875.

[23] Maneiro-Catoira R, Bregains J, Garcia-Naya JA, Castedo L. Enhanced time-modulated arrays for harmonic beamforming. IEEE Journal of Selected Topics in Signal Processing 2017; 11 (2): 259-270. doi: 10.1109/JSTSP.2016.2627178

[24] Maneiro-Catoira R, Bregains J, Garcia-Naya JA, Castedo L. Analog beamforming using time-modulated arrays with digitally preprocessed rectangular sequences. IEEE Antennas and Wireless Propagation Letters 2018; 17 (3): 497-500. doi: 10.1109/LAWP.2018.2797971

[25] Chen K, Yang S, Chen Y, Qu S. Accurate models of time-invariant beampatterns for frequency diverse arrays. IEEE Transactions on Antennas and Propagation 2019; 67 (5): 3022-3029. doi: 10.1109/TAP.2019.2896712

[26] Secmen M, Demir S, Hizal A, Eker T. Frequency diverse array antenna with periodic time modulated pattern in range and angle. In: 2007 IEEE Radar Conference; Boston, MA, USA; 2007. pp. 427-430.

[27] Eker T, Demir S, Hizal A. Exploitation of linear frequency modulated continuous waveform (LFMCW) for frequency diverse arrays. IEEE Transactions on Antennas and Propagation 2013; 61 (7): 3546-3553. doi: 10.1109/TAP.2013.2258393

[28] Rocca P, Oliveri G, Mailloux RJ, Massa A. Unconventional phased array architectures and design methodologies-a review. Proceedings of the IEEE 2016; 104 (3): 544-560. doi: 10.1109/JPROC.2015.2512389

[29] Ni D, Yang S, Chen Y, Guo J. A study on the application of subarrayed time-modulated arrays to MIMO radar. IEEE Antennas and Wireless Propagation Letters 2017; 16: 1171-1174. doi: 10.1109/LAWP.2016.2626478

[30] Rocca P, Poli L, Oliveri G, Massa A. Synthesis of sub-arrayed time modulated linear arrays through a multi-stage approach. IEEE Transactions on Antennas and Propagation 2011; 59 (9): 3246-3254. doi: 10.1109/TAP.2011.2161535

[31] Aksoy E. Harmonic beam steering in 4D linear arrays through pulse difference. In: 22nd Telecommunications Forum (TELFOR'2014); Belgrade, Serbia; 2014. pp. 792-794.

[32] Aksoy E. Harmonic beam steering in time-modulated arrays with simultaneous sidelobe control. In: International Symposium on Fundamentals of Electrical Engineering (ISFEE'2014); Bucharest, Romania; 2014. pp. 1-3.

[33] Yao AM, Wu W, Fang DG. Single-sideband time-modulated phased array. IEEE Transactions on Antennas and Propagation 2015; 63 (5): 1957-1968. doi: 10.1109/TAP.2015.2406890

[34] Poli L, Rocca P, Oliveri G, Massa A. Harmonic beamforming in time-modulated linear arrays. IEEE Transactions on Antennas and Propagation 2011; 59 (7): 2538-2545. doi: 10.1109/TAP.2011.2152323

[35] Li H, Chen Y, Yang S. Harmonic beamforming in antenna array with time-modulated amplitude-phase weighting technique. IEEE Transactions on Antennas and Propagation 2019; 67 (10):6461-6472. doi: 10.1109/TAP.2019.2922815